

# Robust, Basis-Set Independent Method for the Evaluation of Charge-Transfer Energy in Noncovalent Complexes

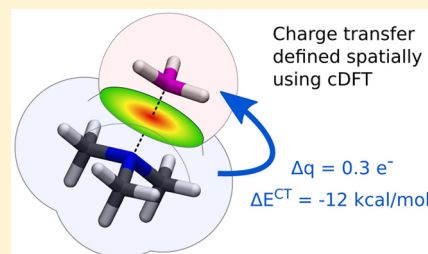
Jan Řezáč<sup>\*,†</sup> and Aurélien de la Lande<sup>‡</sup>

<sup>†</sup>Institute of Organic Chemistry and Biochemistry, Academy of Sciences of the Czech Republic, Flemingovo nám. 2, 166 10 Prague 6, Czech Republic

<sup>‡</sup>Laboratoire de Chimie Physique CNRS UMR 8000, Université Paris-Sud. Bât. 349, 15, rue Jean Perrin, 91405 Orsay Cedex, France

## Supporting Information

**ABSTRACT:** Separation of the energetic contribution of charge transfer to interaction energy in noncovalent complexes would provide important insight into the mechanisms of the interaction. However, the calculation of charge-transfer energy is not an easy task. It is not a physically well-defined term, and the results might depend on how it is described in practice. Commonly, the charge transfer is defined in terms of molecular orbitals; in this framework, however, the charge transfer vanishes as the basis set size increases toward the complete basis set limit. This can be avoided by defining the charge transfer in terms of the spatial extent of the electron densities of the interacting molecules, but the schemes used so far do not reflect the actual electronic structure of each particular system and thus are not reliable. We propose a spatial partitioning of the system, which is based on a charge transfer-free reference state, namely superimposition of electron densities of the noninteracting fragments. We show that this method, employing constrained DFT for the calculation of the charge-transfer energy, yields reliable results and is robust with respect to the strength of the charge transfer, the basis set size, and the DFT functional used. Because it is based on DFT, the method is applicable to rather large systems.



## ■ INTRODUCTION

Computational methods are important tools for the study of noncovalent interactions. The calculations can go beyond reproducing physically observable variables and provide further insights. Useful information can be obtained using methods that allow the decomposition of interaction energy into contributions arising from different physical phenomena. This allows better understanding of the underlying mechanisms as well as quantitative characterization and classification of noncovalent interactions of different nature.<sup>1</sup> Interaction energy is usually decomposed into electrostatic, polarization (induction), exchange (Pauli repulsion), and London dispersion terms. This decomposition can be achieved by means of perturbation theory, where the interaction is treated as a perturbation added on top of calculations of noninteracting monomers,<sup>2,3</sup> or by a stepwise evaluation and relaxation of the separate contributions in a variational calculation of the complex starting from a state constructed from noninteracting monomers.<sup>4</sup>

In addition to these well-defined terms, it is possible to separate other components that can provide important information. One such contribution is the energy associated with charge transfer in noncovalent complexes (this text refers to this quantity as to charge-transfer energy). The concept of charge transfer as a mechanism of noncovalent interactions was described already in 1952 by Mulliken.<sup>5</sup> In charge-transfer complexes (also called donor–acceptor complexes), some electron density (usually a small fraction of an elementary

charge) of the donor molecule D is transferred to the acceptor A. This effect can also be described as a resonant state mixing neutral ( $D \cdots A$ ) and ionic ( $D^+ \cdots A^-$ ) states. The magnitude of the charge transfer is determined mainly by the ionization potential of the donor and the electron affinity of the acceptor and depends strongly on the intermolecular distance and their mutual orientation. In terms of interaction energy, charge transfer leads to an additional stabilization of the complex. Charge transfer is common in inorganic chemistry, occurring in many metal–ligand complexes. Organic charge-transfer complexes are also very important as they impart special properties, including conductivity or semiconductivity, to organic compounds.<sup>6</sup> In addition to complexes with very strong charge-transfer character (referred to as charge-transfer or CT complexes), charge transfer also contributes to other polar interactions, most notably hydrogen bonds.

The concept of charge transfer is easy to understand intuitively but hard to define rigorously or to quantify (both in terms of the amount of the charge transferred and in terms of energy). In the context of the well-defined physical components of interaction energy, charge transfer is part of the polarization term and can be viewed as a very strong polarization where the polarized electron density of one molecule extends into the space occupied by the other one. Therefore, it is not easy to separate the charge transfer from the remaining polarization.

**Received:** October 20, 2014

Although this topic has been discussed for a long time and several approaches had been devised,<sup>7–14</sup> none of them is completely satisfactory.

This difficulty stems from the fact that separating a noncovalent complex into the “molecules” from which it is formed is an artificial construction—from a quantum-mechanical point of view, a noncovalent complex is an inseparable entity described by a single wave function (for this reason, we will refer to the molecules in the complex as to “molecular fragments” from now on). Any approach that divides the electron density of the complex into the densities of the molecular fragments (in order to count the charge on them) relies on an arbitrary choice of the partitioning method, making it possible to obtain arbitrary results. However, if one wants to define charge transfer as a phenomenon separated from intramolecular polarization, such partitioning of the system cannot be avoided. While there is no exact solution, we can try to find a physically meaningful, robust partitioning scheme that will closely reproduce the vague (yet intuitively easy to understand) definition of the charge transfer between the “molecules” in a noncovalent complex.

The existing methods use two different approaches to the partitioning of the electron density in a noncovalent complex, which we will refer to as orbital-based and spatial partitioning. The orbital-based partitioning assigns the electrons to a given fragment if they occupy basis set functions localized on atoms belonging to that fragment. The charge transfer can be then easily defined as the shift of the electron density localized on fragment A to orbitals located on fragment B (while such rearrangement of electron density within a fragment is referred to as polarization). This approach is compatible with commonly used interaction energy decomposition methods (it is utilized in multiple variants of perturbation theory<sup>8,9</sup> and also in the Kitaura–Morokuma decomposition<sup>7</sup> and related methods), but it is not as unambiguous as it seems at first sight. The problem is that the result strongly depends on the basis set used: when utilized with small basis sets, the charge transfer mixes with the basis set superposition error and the charge transfer is overestimated. On the other hand, if one approaches the complete basis set limit, the basis set functions on fragment A can describe even electrons (spatially) located on fragment B and the charge transfer in the orbital-based definition vanishes. This was discussed earlier by Stone<sup>8</sup> in the context of perturbation theory. Although a definition of charge transfer suffers from the problems described above, Stone argues that a reasonable estimate of the charge transfer term can be achieved by calculation in a sufficiently large basis set (so that the effect of the BSSE is negligible) while the atom-centered nature of the basis set makes it possible to separate the charge transfer (because such a basis set located on one fragment still cannot sufficiently describe the orbitals on the other one). However, a method with such a strong basis set dependence can hardly be used when there is no reference available to calibrate this cancellation of errors. In general, the intermolecular perturbation theory offers a more rigorous decomposition of the interaction energy than the variational calculations and is preferred in practical applications. However, there is one more potential issue when the perturbation theory is applied to charge-transfer complexes: its formulation is based on the assumption that the intermolecular interaction is only a small perturbation to the noninteracting molecules. This is, of course, the case in most noncovalent complexes, but it might not be

valid in strong charge-transfer complexes, where large changes in electron density occur.

To avoid the difficulties with the orbital-based definition of molecular fragments, a different approach can be used—a spatial partitioning of the electron density of the complex. Here, electrons can be assigned to the molecular fragments on the basis of their position in space—for example, electron density in any point of space closer to the nuclei of fragment A than to fragment B is attributed to fragment A and vice versa. This approach eliminates the basis set dependence (as long as the basis set used is large enough to provide realistic electron density) but introduces an arbitrary choice of how to divide the space. It is obvious that a certain division may yield zero charge transfer (if such border is drawn that the fragments conserve the charge of noninteracting molecules) or that an arbitrary result can be obtained if another partitioning is used. Additionally, the use of the spatial partitioning in energy decomposition is not as straightforward as in the case of the orbital-based approach. It is easy to calculate the amount of charge transfer by calculating the charge of the fragments (a population analysis based on integrating the electron density over the spatial regions), but obtaining the energy associated with the charge transfer is more complicated.

It has been noted earlier that this energy can be calculated as a difference between the ground state of the complex (where the charge transfer occurs) and another calculation in which the charge transfer is prohibited yet other properties are relaxed. One of the few methods that allow this is the constrained density functional theory (cDFT).<sup>15</sup> The concept of cDFT is now well developed and several implementations are available. In cDFT calculations, the energy is minimized under additional constraints on the charge or spin densities on atoms or fragments, which the optimized electronic density must satisfy. Since atomic charges in molecules are not uniquely defined in quantum mechanics, several alternative partition schemes can be used to define the type of charges (Mulliken, Löwdin, Hirshfeld, ...) to be constrained in a cDFT calculation. Constrained DFT had been already applied to the calculation of charge transfer energies by Wu and co-workers.<sup>14</sup> However, they used a rather simple spatial population scheme integrating the density over Becke cells,<sup>16</sup> which divide the distances between atoms in a fixed ratio. While the authors reported good results for charge transfer in water dimer, such a scheme which does not reflect the actual electron density of the system does work only in systems where the simple geometric partitioning accidentally coincides with the partitioning in which charge transfer is defined well.

This article shall demonstrate that in general, meaningful CT energies can be obtained with cDFT only with specifically designed partition schemes, which must be derived from a reasonable formal definition of the charge transfer. In that case, a charge transfer-free reference state is needed and the natural choice is to build it from the electron densities of the noninteracting fragments. One such a scheme was developed earlier by Wu et al.<sup>17,18</sup> who used it in configuration interaction calculations on states obtained with cDFT (the authors did not tested the partition scheme for calculating CT energies). Here, we implemented two alternative partition schemes, also based on fragment densities, for the calculation of CT energies. We report extensive test calculations with the objective to assess the capability of cDFT to provide robust, meaningful cDFT based CT energies with these partition schemes. The results also indicate that any partitioning scheme satisfying the conditions

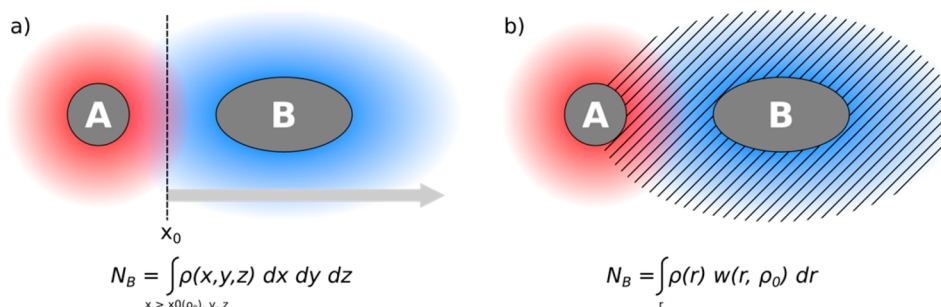


**Figure 1.** Simplified description of the two schemes for defining charge transfer on the basis of a promolecular density constructed by overlapping the electron densities of the isolated fragments. (a) A simple geometrical scheme—a plane at position  $x_0$ —is sought that divides the promolecular density into half-spaces conserving the original charge of the fragments. Then, the charge on molecule B in the complex is obtained by integrating the actual electron density of the complex in the respective half-space. (b) Hirshfeld population analysis based on promolecular reference densities. The integration is carried over the whole space, but each point is multiplied by a weight that describes its contribution to the given fragment; this weight is obtained from the reference densities of the fragments.

that arise from the same definition of charge transfer would yield very similar results.

As a test case, we use a set of small charge-transfer complexes ranging from weak to very strong ones.<sup>19</sup> Our approach has been found to be very robust, exhibiting only weak basis-set or exchange-correlation functional dependence. It is difficult to test the absolute accuracy of the new methodology, because there is no reliable reference available. Nevertheless, we will compare the cDFT-based spatial method with other approaches on a widely used model system, the hydrogen bond in water dimer. Here, the charge transfer is not very strong, but it is a system for which a large amount of data calculated with many different methods has been published.<sup>19,20</sup> Finally, we demonstrate the applicability of our approach to very large complexes. The cDFT methodology adds only a negligible overhead to standard DFT calculations and thus makes it possible to study rather large systems.

Although there is no benchmark that would allow us to assess the accuracy of the proposed method directly, a comparison of our new results with several other approaches suggests that the new cDFT-based methodology allows a quantitative evaluation of the contribution of the charge transfer to the interaction energy.

## 1. THEORY

**1.1. Definition of Charge-Transfer Energy.** This work focuses on the contribution of the charge transfer to the interaction energy, shortly charge-transfer energy, labeled as  $\Delta E^{\text{CT}}$ . This quantity will be defined as the energy difference of the supramolecule (the noncovalent complex) with a fully relaxed electronic density ( $\rho$ ) and with a relaxed density but with the charge transfer between the fragments prevented. In this article, the required energies will be calculated at the DFT level, but this concept is general and can be implemented in other methods as well. The energy of the fully relaxed system ( $E^{\text{DFT}}$ ) is obtained by a standard DFT calculation while the energy of the charge-transfer prevented system is obtained by constrained DFT ( $E^{\text{cDFT}}$ ).

$$\Delta E^{\text{CT}} = E^{\text{DFT}} - E^{\text{cDFT}} \quad (1)$$

$E^{\text{cDFT}}$  is obtained by the minimization of the energy functional given by eq 2, in which  $\lambda_c$  is a Lagrange multiplier and  $w$  is a function of the real space that determines the constraining property, in this case, a function defining the charge of the molecular fragments. The charge can either be calculated for

the whole fragment or expressed as a sum of atomic charges obtained using any population analysis method.

$$E^{\text{cDFT}}[\rho, \lambda_c] = \min_{\rho} \max_{\lambda_c} (E^{\text{DFT}}(\rho) + \lambda_c (\int \rho(r) w(r) dr - N_c)) \quad (2)$$

Algorithms for solving the Kohn–Sham equations resulting from this energy functional have been described in various articles or book chapters, and we refer the interested reader to these publications for additional details.<sup>21–23</sup>

**1.2. Definition of the Weight Function for the cDFT Calculations of Charge Transfer.** A critical issue in cDFT is to choose practical mathematical definitions for the function  $w$ . Such definition depends on the type of atomic charges one wishes to constraint. For example,  $w$  can be defined such that the integration of the product  $\rho(r)w(r)$  over space gives the sum of the Hirshfeld charges of the atoms subjected to the constraint. In the Hirshfeld scheme,<sup>24</sup> the value of the function  $w$  at point  $r$  is given by

$$w(r) = \frac{\sum_{i=1}^{N_{\text{at}}} \rho_i^a(r) \delta_i}{\sum_{j=1}^{N_{\text{at}}} \rho_j^a(r)} \quad (3)$$

where  $\rho_i^a$  is the electron density of the neutral isolated atom and  $\delta_i$  is a binary function equal to 1 if atom  $i$  is included in the constrained domain and equal to 0 otherwise. The sums run over all the atoms ( $N_{\text{at}}$ ).

Alternatively, if using the LCAO (Linear Combination of Atomic Orbitals) framework, the elements of the matrix representing the function  $w$  can be defined such that the electronic density is constrained according to the Mulliken<sup>25</sup> or Löwdin<sup>26</sup> definitions of charges. Our preliminary tests showed that none of the readily available population schemes (Mulliken, Löwdin, Becke,<sup>16</sup> Hirshfeld,<sup>24</sup> Voronoi deformation density<sup>27</sup>) permit a reliable estimation of charge-transfer energy by cDFT (see the Results section). In order to quantify charge-transfer energies reliably, special attention has to be paid to defining the function  $w$ . The charge transfer should be defined only relative to a reference state that is free of charge transfer. A natural choice is to start from isolated (infinitely separated) molecules. Not only is it a physically sound choice, but the electron density of such a system can be calculated easily. The next step is the formation of the complex, bringing the noninteracting fragments to a contact distance. In practice, electron densities of the isolated molecules (in the geometry



that they have in the complex) are superimposed onto the geometry of the complex, giving rise to the so-called promolecular density. The promolecular electron density does not correspond to any real electronic state of the complex, but it has an important property: the densities are not polarized, and thus, there is no charge transfer. Because the noncovalent interaction introduces only a small perturbation to the covalent electronic structure of the fragments, such a state is also a good approximation of the relaxed density of the complex.

Our objective is therefore to define the function  $w$  in such a way that after the optimization of the cDFT energy functional, the fragments conserve the charges that they had in the promolecular density. Although such partitioning schemes are not unique, we will show that different formalisms satisfying the condition of conserving the charge of the fragments in the starting frozen density lead to practically identical results, which is an important proof of the robustness of our approach. We have developed two such schemes, a simple geometrical one, which serves as a proof of the concept, and a more advanced, universally applicable one, which is based on the Hirshfeld population analysis. Their main principles are outlined in Figure 1.

The first formalism of the partitioning scheme to be discussed is very simple and applicable only to the CT complexes with geometry close to linear. We refer to this scheme as to an optimized-plane (OP) approach. Consider a linear noncovalent complex (Figure 1). The promolecular electron density is constructed from DFT calculations of the isolated monomers, and it is partitioned by a plane perpendicular to the intermolecular axis positioned at distance  $r$  from one of these atoms. The value of  $r$  is optimized so that the integration of the promolecular electron density on each side of the plane leads to unchanged charges for the fragments with respect to the infinitely separated situation. The optimization procedure involves a scan in  $r$ ; at each point, the fragment charges are evaluated on the promolecular density. The obtained set of values is interpolated by a polynomial, and the position  $r_{\text{opt}}$  where it evaluates to zero is obtained analytically. This procedure has been automated using the Cuby framework.<sup>28</sup> Then, the constraint in a cDFT calculation is defined by the  $w$  function:

$$w(r) = \begin{cases} 1 & \text{for } r < r_{\text{opt}} \\ 0 & \text{for } r \geq r_{\text{opt}} \end{cases} \quad (4)$$

In eq 2,  $N_c$  is set to the number of electrons of the left-hand-side fragment. With this prescription, the relaxed electronic density obtained by the minimization of eq 2 will preserve the charge of the left-hand-side fragment (and thus also for the right-hand-side fragment since the total number of electrons is also imposed in the KS procedure). While this scheme is adapted for simple geometries, it might not be satisfactory when the plane dissecting the intervening space between the fragments does not coincide with the region of the low electron density between them.

A more advanced, general scheme can be devised following the spirit of the Hirshfeld partitioning scheme but using the electron densities of the noninteracting fragments ( $\rho_A$  and  $\rho_B$ ) as references instead of the densities of the isolated neutral atoms (such as in eq 3). This Hirshfeld population analysis based on molecular-fragment reference densities is abbreviated as  $H_M$ , in contrast to the original approach, using atomic reference  $H_A$ . In this case, the weight function  $w$  reads:

$$w(r) = \frac{\rho_A(r)}{\rho_A(r) + \rho_B(r)} \quad (5)$$

Now,  $w$  is not binary (the function  $w$  being 1 or 0) as in the plane-based scheme, but again, the fragments will retain their charges after the optimization of the cDFT energy under the constraint. Unlike the previous case, this approach can be used for noncovalent complexes of any shape.

## 2. METHODS AND COMPUTATIONAL DETAILS

**2.1. Constrained DFT Calculations.** Constrained DFT calculations have been performed with a locally modified version of deMon2k.<sup>29</sup> This software solves the Kohn–Sham equations within a representation of the KS MO as linear combination of Gaussian-Type atomic orbitals. It implements local density approximation (LDA), generalized gradient approximation (GGA) and meta-GGA DFT functionals. We have previously reported the details of the implementation of the method in deMon2k.<sup>30</sup>

For the present study, new mathematical expressions have been implemented for the calculation of the weight matrix elements adapted for charge-transfer energies. The weight matrix elements  $W_{\mu\nu}$  ( $\mu$  and  $\nu$  are the indexes of atomic orbitals  $\varphi$ ) are calculated numerically on a grid of points with coordinates  $r_i$ :

$$W_{\mu\nu} = \sum_i a_i(r_i) \varphi_\mu(r_i) \varphi_\nu(r_i) w_i(r_i) \quad (6)$$

where the coefficients  $a_i$  are the integration weights. The terms  $w_i(r_i)$  are given by eqs 4 (OP approach) and 5 ( $H_M$ ). In the former case, preliminary calculations are performed to determine the optimized position of the separating plane and cDFT then requires the value of  $r_{\text{opt}}$  in the input. In the latter case, separately calculated densities of the isolated fragments are required to compute  $w(r)$ ; these are carried out automatically prior to the actual cDFT calculation, and the relevant density coefficients are stored in memory. To reduce memory requirements, we do not store the orbital density matrices of the isolated fragments but instead the auxiliary densities ( $\tilde{\rho}$ ) used by deMon2k to calculate the Coulomb potential. These variationally fitted auxiliary densities are expressed as linear combinations of Hermite Gaussian functions. This simplification is justified, because the reference densities are only used to define integration weights in eq 5 and are not integrated by themselves in the present framework. Note that in our implementation the user has the option to choose any arbitrary charge and spin-state multiplicity for the fragments.

All the cDFT calculations have been performed with adaptive grids of fine accuracy to integrate the exchange-correlation energy potential.<sup>31</sup> We have used the auxiliary basis set GEN-A2\* to expand the auxiliary densities for the computation of the coulomb potential.<sup>32</sup> For GGA functionals, the auxiliary density was also used to calculate the exchange-correlation potential.<sup>33</sup>

**2.2. Other Calculations.** The DFT calculations with natural bond orbital (NBO) population analysis<sup>13</sup> were performed in Turbomole 6.5.<sup>34,35</sup> In the study of the convergence of the CT energy with the basis set size, we evaluated also the basis set superposition error (BSSE), calculated as a difference between the interaction energy calculated without and with a counterpoise correction.<sup>36</sup> To test the performance of the proposed methodology, we have

used a set of small model complexes developed previously by Karthikeyan et al.<sup>19</sup> This set contains 11 systems covering a wide range of charge transfer from weak (0.01 of an electron transferred according to NBO population analysis) to very strong (0.33 of an electron transferred). For this work, we have recalculated the counterpoise-corrected CCSD(T)/CBS interaction energies to create a new benchmark-data set compatible with other data sets that one of the authors developed.<sup>37,38</sup> The composite CCSD(T)/CBS results consist of HF/aug-cc-pVQZ energy, MP2 correlation energy extrapolated<sup>39</sup> to the complete basis set limit from aug-cc-pVTZ and aug-cc-pVQZ calculations and the  $\Delta\text{CCSD(T)}$  correction (the difference between CCSD(T) and MP2) calculated in the cc-pVTZ basis set with diffuse atoms on all but hydrogen atoms (the so-called heavy-augmented basis set). More details on this computational setup and its accuracy can be found in our recent papers.<sup>37,40,41</sup> These calculations were performed in Molpro version 2010.<sup>42</sup> DFT interaction energies to be compared with the benchmark were calculated in the def2-QZVP basis set and augmented with the D3 empirical dispersion correction<sup>43</sup> with Becke–Johnson damping.<sup>44</sup> Unless explicitly noted, all DFT calculations presented here were performed in the PBE functional.

Additionally, more thorough analysis has been performed for water dimer, because it is a system in which charge transfer was extensively studied in the past. The geometry of the water dimer has been taken from the S66 data set.<sup>37</sup>

### 3. RESULTS AND DISCUSSION

We begin the discussion with a thorough examination of the proposed method with respect to its dependence on the basis set and DFT functional used. Subsequently, the results are compared with several other approaches for the quantification of the charge-transfer effects. Finally, an application of the method to a calculation of the charge transfer between tetracyanoethylene (an electron acceptor) and a graphene model of increasing size shows that this approach is applicable even to large systems.

**3.1. Benchmark Calculations and Interaction Energies.** To set the most accurate benchmark, we recalculated the CCSD(T)/CBS interaction energies in the test set in basis sets larger than the ones used in the original work. The differences are small (4% on average); the main reason for recalculating the test set was to make it fully compatible with our other data sets (e.g., S66 and X40 sets<sup>38,40</sup>) calculated at this level. The details on the composite CCSD(T)/CBS calculations are given above. The results are presented in Table 1.

It is known that DFT (after correcting for London dispersion) overestimates the interaction energies in complexes with strong charge-transfer character because of the overdelocalization of the electron density due to the self-interaction error.<sup>45</sup> This improves when hybrid functionals including exact exchange are used. However, the code on which we have based our cDFT implementation, deMon2k, does not support them. We have tested several functionals (calculated in the def2-QZVP basis set, with D3 dispersion correction), comparing the interaction energies with the CCSD(T)/CBS benchmark. The average unsigned errors (the relative error in parentheses is calculated as the average error divided by the average interaction energy in the set) are 2.6 kcal/mol (19%) for PBE, 13.7 kcal/mol (99%) for B-LYP, 4.1 kcal/mol (29%) for PW91, and 2.2 kcal/mol (16%) for TPSS. Since TPSS is a meta-GGA functional, which cannot take full advantage of the auxiliary density formalism in deMon2k, we have decided to use

**Table 1. Set of Charge-Transfer Complexes Used in This Work, Their CCSD(T)/CBS Interaction Energies, and the Best Estimate of the Charge-Transfer Energy Obtained with Our cDFT Approach Using the Hirshfeld Population Scheme Based on Molecular-Fragment Density in the def2-QZVPPD Basis Set<sup>a</sup>**

	system	$\Delta E^{\text{int}}$ , CCSD(T)/CBS	$\Delta E^{\text{CT}}$ , cDFT
1	C <sub>2</sub> H <sub>4</sub> ...F <sub>2</sub>	−1.02	−1.42
2	NH <sub>3</sub> ...F <sub>2</sub>	−1.71	−2.53
3	C <sub>2</sub> H <sub>2</sub> ...ClF	−3.91	−1.95
4	NH <sub>3</sub> ...Cl <sub>2</sub>	−4.91	−4.41
5	HCN...ClF	−4.77	−0.89
6	H <sub>2</sub> O...ClF	−5.20	−2.74
7	NH <sub>3</sub> ...SO <sub>2</sub>	−5.72	−2.84
8	NH <sub>3</sub> ...ClF	−11.16	−9.65
9	NMe <sub>3</sub> ...SO <sub>2</sub>	−14.83	−14.17
10	NH <sub>3</sub> ...BH <sub>3</sub>	−44.27	−11.99
11	NMe...BH <sub>3</sub>	−55.33	−11.62

<sup>a</sup>Values in kcal/mol.

the PBE for our calculations although the results are slightly worse. In all these cases, the strength of the interaction is overestimated. As a result, the charge-transfer energies reported here are probably overestimated as well. This error is hard to quantify as there is no reliable reference, but the stability of the CT energies with respect to the DFT functional used (see Section 3.4) suggests that the error might be smaller than the one in overall interaction energies. Hybrid functionals are planned to be added for a future release of deMon2k;<sup>46</sup> we will revisit our CT calculations once we have implemented cDFT in the new version.

**3.2. Models for the Spatial Definition of Charge Transfer.** We have developed two new models for the partitioning of the noncovalent complex, a simple one using a plane perpendicular to the intermolecular axis (the OP scheme) and a more general one based on the Hirshfeld scheme with noninteracting molecular-fragment densities as reference ( $H_M$ ). In the linear complexes, where the plane separation is applicable, both approaches should yield approximately the same results, provided that the basis set is large enough for an accurate description of the constrained state.

To demonstrate this equivalence, we have selected two model complexes—the water dimer, representing a weak charge-transfer system, and the NH<sub>3</sub>...ClF complex, where charge transfer is rather strong. In these systems, charge-transfer energy was evaluated using both models in an extensive series of basis sets ranging from split valence to quintuple-zeta. The charge-transfer energies are plotted in Figure 2. The basis sets are ordered by decreasing values of the basis set superposition error, which serves as a good measure of the convergence of the calculation with respect to the basis set size.

In smaller basis sets, the two models follow the same trends (for the NH<sub>3</sub>...ClF complex, the two calculations in the smallest basis set and OP partitioning did not converge). In large basis sets, the results became practically equivalent.

In the next step, we compared these two approaches over the whole test set of CT complexes. Again, we observed very good agreement (see the two series plotted in red in Figure 3); the average difference is only 0.4 kcal/mol. These results suggest that different partitioning schemes satisfying the condition that we use to define the charge transfer (it is the zero charge transfer in the superimposed densities of noninteracting

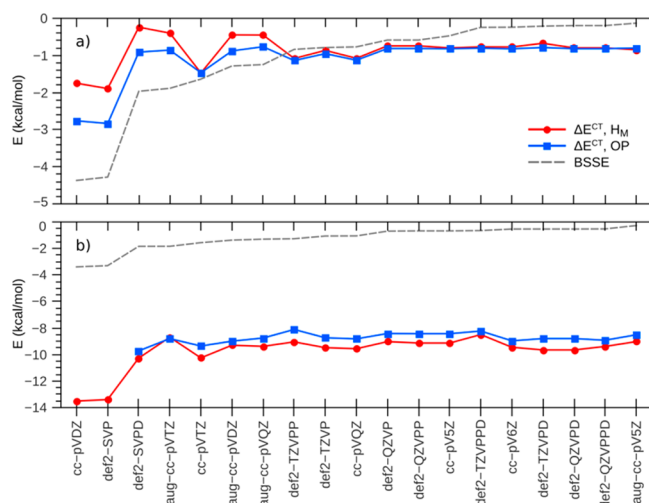


**Figure 2.** Charge-transfer energy in (a) water dimer and (b)  $\text{NH}_3 \cdots \text{ClF}$  complex obtained using the cDFT methodology based on the plane separation of the molecular fragments (OP, blue) and their definition based on the Hirshfeld population scheme ( $H_M$ , red), calculated in a series of basis sets. To indicate the basis set convergence, the basis set superposition error is plotted in addition (gray, dashed). Values in kcal/mol.

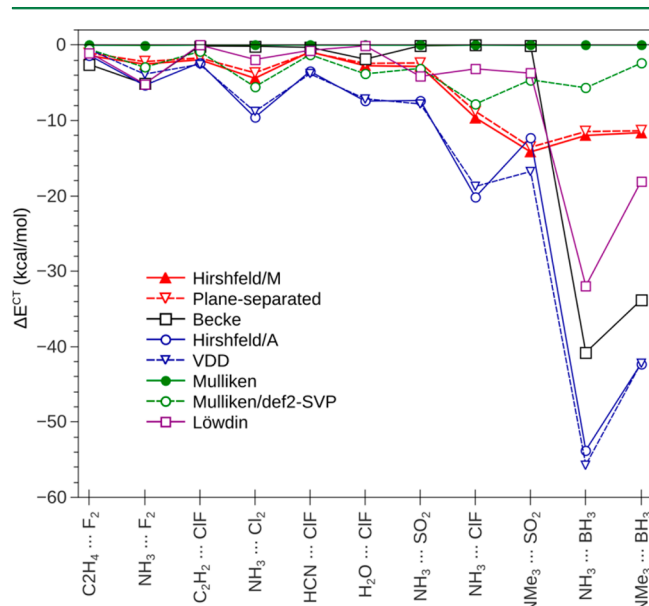


**Figure 3.** Charge-transfer energies calculated using cDFT constraints expressed in terms of various population analysis methods. The red lines represent the two approaches introduced in this paper: Hirshfeld population analysis based on molecular-fragment densities  $H_M$  and the separation of the fragments by a plane in an optimized position (OP). All calculations have been performed in the def2-QZVPPD basis set unless indicated otherwise.

fragments) lead to similar results. In the following text, we will discuss only the Hirshfeld partitioning, as it is a more universal scheme, which can be used in systems with arbitrarily complex geometries.

To highlight the difference between the schemes designed specifically to describe charge transfer and other cDFT approaches where the constraints are defined in terms of commonly used population schemes, we calculated the CT energies in the test set. The CT energies are calculated as

outlined above, constraining the charge of the fragments to the charge of the respective isolated molecule (it is to zero in these cases). The results are plotted in Figure 3; the calculated values can be found in Table S1 in the Supporting Information. A large def2-QZVPPD basis set was used unless noted otherwise.

The simplest example of space-based constraint is the use of the Becke charges,<sup>16</sup> which are obtained by assigning the electron density at each point to the nearest atom (more exactly, by integration over Becke cells). This approach treats all the atoms as having the same radius, and the separation of the molecular fragments therefore does not reflect their actual spatial extent. As a result, the CT energies are practically random (from close to zero to strongly overestimated), depending on how the geometric partitioning matches the one optimal for the description of CT. It should be noted that in different implementations, the Becke cells can be scaled with atomic radii in order to get a more realistic partitioning. We have briefly tested this approach as well but it does not bring any substantial improvement.

A more realistic description of the fragments can be achieved with the original Hirshfeld partitioning<sup>24</sup> (eq 3), which is based on estimated promolecular densities constructed as a superposition of the densities of free, spherically averaged neutral atoms ( $H_A$ ). However, this description is still approximate as it neglects the rearrangement of the electron density in the molecule and the results exhibit large errors as compared to the  $H_M$  scheme. In the weaker complexes, the results follow the same trends as in the fragment density-based schemes and the CT energies are overestimated by a similar factor. Only in the two strongest complexes, the error is much larger as the difference between proatomic and promolecular densities become more severe. The scheme based on the Voronoi deformation density<sup>27</sup> populations yields practically the same results, because it is based on the same promolecular density as  $H_A$ , only the integration is carried out over separate cells.

When Mulliken charges<sup>25</sup> are used to define the constraint, the method becomes orbital-based, because the assignment of electron density to the fragments is based on to which atom the respective atomic orbital belongs. Figure 3 shows the plotting of the CT energies obtained with Mulliken population constraints calculated in two basis sets, small def2-SVP and large def2-QZVPPD. In the small basis set, the energies are of reasonable magnitude, but the calculations fail to identify the strongest CT. When we pass to the large basis set, the CT energies become practically zero. This is in line with the expectations for orbital-based schemes. Another orbital-based approach is the Löwdin population analysis.<sup>26</sup> In this case, the formalism is more complex and leads to nonsystematic charge-transfer energies that do not vanish when the basis set size increases.

Overall, it is clear that the only way to describe charge transfer in the cDFT framework reliably is to use a constraint developed specifically for this purpose, one that reflects the actual electronic structure of the molecular fragments and preserves their charges in a noninteracting reference state. The two schemes satisfying this condition that we have designed use different formalism, yet they lead to practically identical charge-transfer energies. This is an important proof of the robustness of the approach. On the other hand, the large differences between CT energies obtained with different population schemes show that this quantity is very sensitive to the choice of the scheme.



### 3.3. Basis Set Dependence of Charge-Transfer Energy.

First, we analyze the basis set dependence of the two model complexes, water dimer and  $\text{NH}_3 \cdots \text{ClF}$ , in detail. The charge-transfer energies are plotted in Figure 2. The calculations in the smallest (double- $\zeta$ ) basis sets are compromised by two factors: first, by the ability of the basis set to describe the electronic structure of both the constrained and relaxed states and, second, by the basis set superposition error (which is plotted in Figure 2 along with the charge-transfer energies). On the other hand, the charge-transfer energies become stable in triple- $\zeta$  basis sets although the BSSE is not negligible yet. Unlike the orbital-based approach, where the BSSE is by definition removed in the constrained calculation, here, it occurs in both calculations, and therefore, it (at least partially) cancels out. Regarding the charge-transfer energies themselves, it is clear that they converge to a finite value, contrary to the orbital-based definitions, where the charge transfer decreases with the basis set size and vanishes completely at the CBS limit.

Second, we turn to the complete test set. Here, we have utilized a smaller subset of our series of basis sets: correlation-consistent basis sets with diffuse functions<sup>47</sup> aug-cc-pVXZ ( $X = \text{D, T, Q}$ ), used widely for the calculations of noncovalent interactions, and the Ahlrichs triple- $\zeta$  basis set def2-TZVP, optionally with additional polarization (def2-TZVPP) and diffuse functions (def2-TZVPD),<sup>48</sup> because these basis set performed well in our previous tests. The charge-transfer energy is compared to benchmark calculations in the large def2-QZVPPD basis set (the CT energies at this level are listed in Table 1). The average errors computed in the test set are listed in Table 2.

**Table 2. Mean Unsigned Error of Charge-Transfer Energies in the Test Set Calculated in Different Basis Sets<sup>a</sup>**

basis set	MUE (kcal/mol)	
	all	without $\text{BH}_3$
aug-cc-pVDZ	0.69	0.55
aug-cc-pVTZ	0.43	0.22
aug-cc-pVQZ	0.40	0.17
def2-TZVP	0.29	0.21
def2-TZVPP	0.24	0.15
def2-TZVPD	0.18	0.18
def2-QZVP	0.25	0.24

<sup>a</sup>The third column lists the error in the set without the complexes of  $\text{BH}_3$ .

It is clear that the aug-cc-pVDZ basis set is too small for an accurate description of the charge-transfer energy, but all the larger basis sets yield very good results. In the series of correlation-consistent basis sets, the errors decrease with the basis set size as expected, but the error in aug-cc-pVQZ is surprisingly large. The def2- family of basis sets generally performs better, but it is obvious that the best results can be achieved only when diffuse functions are added. The surprising difference between the quadruple- $\zeta$  basis sets is caused by rather large and systematic errors of the aug-cc-pVQZ calculations of the two complexes of borohydride ( $\text{BH}_3 \cdots \text{NH}_3$  and  $\text{BH}_3 \cdots \text{trimethylamine}$ ). When these are removed from the set, the error, shown in the last column of Table 2, significantly decreases (the same applies to aug-cc-pVTZ). To investigate this issue further, we performed another test using the polarization-consistent<sup>49</sup> quadruple- $\zeta$  basis set aug-pc-3. The use of a basis set from a different family provides an

independent basis for a comparison of the correlation-consistent and def2- basis set families. The results obtained in this basis set are very close to the def2-QZVPPD benchmark (MUE 0.22 kcal/mol), which suggests that the issue is caused by a problematic description of the  $\text{BH}_3$  complexes in the correlation-consistent basis sets.

Overall, it is clear that, in terms of basis set dependence, the spatial definition provides a very robust description of charge transfer. Once the basis set is large enough to describe the system well and make the BSSE reasonably small, the charge-transfer energy is stable and does not change significantly over a wide range of basis sets from triple- $\zeta$  on. Among the basis sets tested, the def2-TZVP basis set is the smallest reliable one that can be recommended for calculations in larger systems. The accuracy can be further improved by the addition of diffuse functions, which provide a better description of the intermolecular region.

### 3.4. Dependence of Charge-Transfer Energy on the DFT Functional Used.

The results of DFT calculations are often sensitive to the choice of the functional, and in the studied systems, the overall interaction energies vary significantly. To test this dependence in the calculations of charge-transfer energy only, we compare the results obtained with different functionals in our test set in the def2-TZVP basis set. We have chosen several widely used GGA functionals, PBE, B-LYP, and PW91, and the meta-GGA functional TPSS. Note that there is no benchmark against which different functionals can be validated; we express the results in comparison to the average over these four functionals. The average of absolute deviations over the set is reported; it is 0.07 kcal/mol for PBE, 0.17 kcal/mol for B-LYP, 0.10 kcal/mol for PW91, and 0.17 kcal/mol for TPSS. The differences among the functionals are very small. These results suggest that it is safe to use any of them for the charge-transfer calculations; we chose PBE because it yields the best overall interaction energies among the GGA functionals tested.

### 3.5. Correlation of Charge-Transfer Energy and the Amount of Charge Transferred.

An important point to investigate is how charge-transfer energy relates to the amount of charge transferred. The latter quantity is often used as a measure of charge transfer, as it can be easily obtained from a population analysis. In Figure 4, we plot the charge-transfer energy obtained at the PBE/def2-QZVPPD level using the  $H_M$  constraints against the amount of charge transferred as calculated using various population schemes at the same DFT level and from HF/cc-pVTZ calculations (the HF results were taken from ref 19).

The charge-transfer energy indeed correlates best with the charges obtained using the scheme that defined the constraints in the cDFT calculations, the Hirshfeld population analysis based on fragment densities. However, the correlation is not perfect, because the charge-transfer energy is determined not only by the amount of charge transferred but also by the energies of the donor/acceptor orbitals and the changes in other properties of the interacting molecules. These effects are more pronounced in the weaker CT complexes, and the dependence is more linear in the stronger ones. On the other hand, there are no outliers and the charge-transfer energy can thus be expressed as a linear function of the amount of charge transferred, which can be used for a semiquantitative estimation of the CT energy.

The Mulliken and NBO charges exhibit a similar dependence, but outlying points are present. These are the complexes

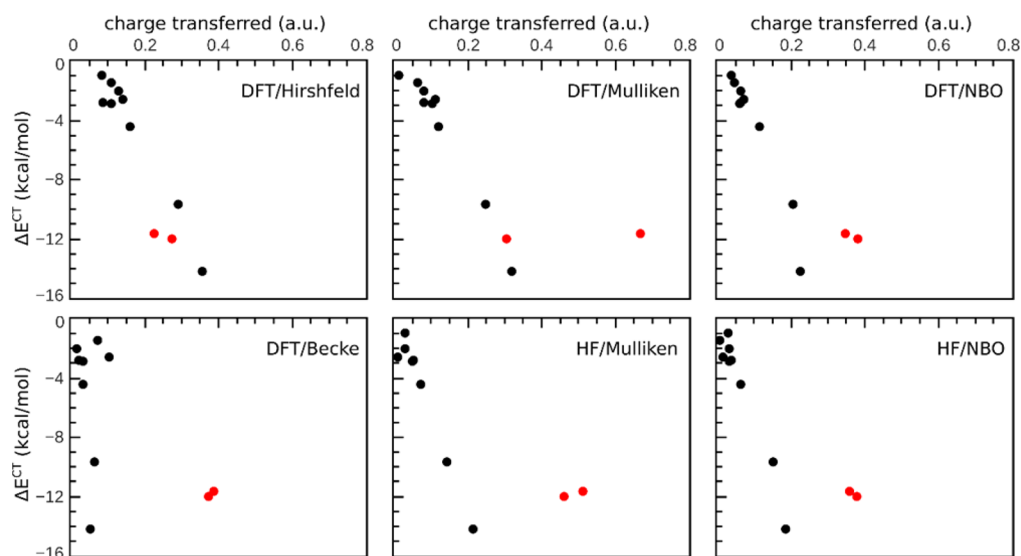


**Figure 4.** Correlation between the amount of the charge transferred (calculated using various population schemes) with the best estimate of the charge-transfer energy calculated using the cDFT approach in the test set of 11 charge-transfer complexes. The complexes of  $\text{BH}_3$  are shown in red.

of  $\text{BH}_3$ , shown in red in the plots. The results obtained from DFT and HF calculations are similar, but the slope of the line is different. Finally, the Becke charges, calculated using a spatial population analysis integrating the charge over Becke cells,<sup>16</sup> yield the worst correlation with the CT energy. This is no surprise as the Becke cells do not account for the actual electron density distribution (moreover, the approach treats all the atoms as having the same diameter), which leads to an unphysical boundary between the molecular fragments.

**3.6. Comparison with Other Approaches—Water Dimer.** Water dimer is often the first model system discussed in many studies on the role of charge transfer in noncovalent interactions. It has been studied by practically all methods that aim to isolate the  $\Delta E^{\text{CT}}$  term, and the results are available in the literature. Although the contribution of charge transfer is not very strong in this case, the abundance of the results published makes it the first choice for the evaluation of any novel methodology. A comprehensive overview of the methods applied to CT energy calculations in water dimer has been published recently,<sup>20</sup> summarizing the results in Table 1 therein. Neglecting the NBO approach, which apparently overestimates the CT energy ( $\Delta E^{\text{CT}} = -9.2$  kcal/mol), all the values fall into the range from  $-0.6$  to  $-1.8$  kcal/mol with a median of  $-0.84$  kcal/mol. The charge displacement analysis described in that work yields an estimate of the charge-transfer energy of  $-0.84$  to  $-0.88$  kcal/mol. Similarly, the most advanced approach available in the literature, the energy decomposition analysis based on absolutely localized orbitals (ALMO-EDA) at the CCSD level,<sup>10</sup> yields a result of  $0.85$  kcal/mol. Although there is no true benchmark as the CT energy is not a rigorously defined quantity, these results suggest that its value for the water dimer lies most likely somewhere around these values. The cDFT-based approach in the def2-QZVPPD basis set yields a CT energy of  $-0.79$  and  $-0.82$  kcal/mol using the  $\text{H}_\text{M}$  and OP schemes, respectively. We can therefore conclude that the present method yields charge-transfer energy that is in good agreement with the best results published so far.

When other population schemes are used in the cDFT calculations of CT energy, the results follow the trends discussed above in Section 3.2. The use of the Mulliken population constraint in the def2-QZVPPD basis set yields zero

$\Delta E^{\text{CT}}$ . On the other hand, the other population schemes lead to overestimated CT energies: Becke  $-18.5$  kcal/mol, Löwdin  $-6.5$  kcal/mol, Hirshfeld using atomic promolecular density  $-11.0$  kcal/mol.

The failure of the Becke population constraint can be illustrated easily by a closer look at how the complex is divided. In complexes with such a simple geometry as the water dimer, the border between the molecular fragments is, in fact, the border between the Becke cells of the two atoms in the closest contact: in this case, hydrogen from one molecule and oxygen from the other. The fragments are thus separated by a plane perpendicular to the axis formed by these two atoms positioned in the middle between them (50% of their distance). Because these two atoms have very different sizes, this position is far from the optimal one and the plane dissects a region with rather high electron density belonging to the oxygen. In our approach using the optimized plane position, it is located substantially closer to the hydrogen at 33% of the interatomic distance.

**3.7. SAPT Charge-Transfer Calculations.** The symmetry-adapted perturbation theory<sup>3</sup> (SAPT) makes it possible to separate the charge-transfer energy as a difference between the calculations where the monomers are calculated in monomer and dimer basis sets.<sup>9</sup> This functionality has recently become available in the PSI4 software package.<sup>50</sup> We attempted to calculate the charge transfer energies using this code at several levels of the SAPT theory up to partial third order perturbation theory (SAPT2 + 3).<sup>51</sup> Since SAPT describes the charge transfer in the terms of orbitals, we investigated also the dependence of the results on the size of the basis set discussed above.

However, we found that, at least in the present implementation, the SAPT methodology does not yield dependable results. In the strongest CT complexes, SAPT not only overestimates the CT energy but, in some cases, it also yields incorrect total interaction energies. It is possible that, in such systems, the approximations involved in the SAPT methodology and the limited order of the perturbation theory are not sufficient for describing the intermolecular interaction as a perturbation to the noninteracting reference state. Although we can not use these calculations as a benchmark for our cDFT approach, we attach the results produced and our



discussion of them as a Supporting Information for those readers who might be interested in the details.

**3.8. Application to the Tetracyanoethylene...Nano-graphene Complex.** Since the approach proposed here is based on DFT, one of its noticeable advantages is its low computational cost. When constrained DFT is efficiently implemented,<sup>30</sup> the overhead introduced by the optimization of the constraining potential (see eq 2) is small and does not affect the scaling with system size. The computation of charge-transfer energies in large molecular systems is therefore accessible with the present scheme. The analysis of basis set dependence also suggests that a triple- $\zeta$  basis set already yields results very close to those obtained with much larger basis sets.

To demonstrate the applicability of our method to large systems, we report a series of complexes of tetracyanoethylene (TCNE) with benzene, coronene, and circumcoronene. This system serves as a model for the study of the role of charge transfer in the adsorption of strong electron acceptors on graphene.<sup>52</sup> The results of  $H_M$  cDFT calculations in the def2-TZVP basis set and DFT-D3 interaction energies calculated at the B-LYP/TZVPP level are summarized in Table 3. While the

**Table 3. Series of Complexes of Tetracyanoethylene with Aromatic Electron Donors of Increasing Size<sup>a</sup>**

electron donor	atoms	$\Delta E^{\text{int}}$ (kcal/mol)	CT (au)	$\Delta E^{\text{CT}}$ (kcal/mol)
benzene	22	−8.8	0.10	−1.4
coronene	46	−14.5	0.18	−2.0
circumcoronene	82	−20.1	0.36	−5.4

<sup>a</sup>The interaction energy was calculated using DFT-D3; charge transfer (CT, as a fraction of the electron transferred) and the associated CT energy were calculated using the presented cDFT/ $H_M$  methodology.

increase in the total energy between the complexes of TCNE with benzene, coronene, and circumcoronene is about the same, the charge transfer grows more rapidly upon the transition from coronene to circumcoronene. This is consistent with a previously published analysis of the structure of the orbitals involved in the charge transfer,<sup>52</sup> HOMO of the graphene and LUMO of tetracyanoethylene. In the case of circumcoronene (unlike both smaller and larger graphene flakes), these orbitals have a matching symmetry that maximizes the charge transfer.

The largest system is a nice example for the demonstration of the computational cost of cDFT CT calculations. It consists of 82 atoms, out of which only 18 are hydrogens, which converts to 2412 basis set functions when the def2-TZVP basis set is used. The cDFT calculation took 30 h on a single processor, which is about twice as much as unconstrained DFT; this time, however, it includes the calculations of the two separate monomers used to define the reference density.

## CONCLUSIONS

We present a novel approach to calculating the energy associated with intermolecular charge transfer (charge-transfer energy,  $\Delta E^{\text{CT}}$ ). This component of interaction energy is calculated as the difference between a standard DFT calculation (with full relaxation of the electron density) and a calculation in which charge transfer between the molecular fragments is prohibited by means of the constrained DFT methodology.<sup>14</sup> The novelty of the present approach is the definition of the constraint in an intuitive, physically sound way, using the electron density of the isolated monomers as a reference state

in which no charge transfer occurs. Such a constraint is unique for each system and makes it possible to find the least perturbed state in which charge transfer is not allowed. Besides a simple geometrical scheme used as a proof of concept, we extended the Hirshfeld population scheme to use the densities of the noninteracting fragments obtained from separate DFT calculations. This makes our approach applicable even to systems with complex geometries. Other schemes would also be suitable for calculating CT energies as long as they make it possible to preserve in the cDFT calculation the charge that the fragments have in the promolecular density. For example, Voronoi (or Becke) deformation density schemes with isolated fragment reference densities introduced<sup>53,17,18</sup> should also be adequate for charge-transfer energy calculations.

It must be noted that there is no objective benchmark against which our results could be validated. The charge transfer is not a directly observable effect—it is an artificial construct built on the intuitive but unphysical idea that the noncovalent complex is separable into the molecules of which it consists. Since there is no objective prescription how to separate the fragments, various methodologies use different formal definitions of the charge transfer and may yield different results. Nevertheless, we are confident that our new approach follows the concept of charge transfer as it is generally understood as closely as possible and that it yields a reasonable quantitative estimate of the energetics of charge transfer.

We have tested the new approach in a wide variety of systems and found it to be very robust, yielding reliable results over a wide range of basis sets and DFT functionals. It is especially important that the results do not change with the basis set size (as long as the basis set is large enough to describe the system well). This is an inherent advantage of the spatial definition of the molecular fragments, in contrast to the calculations defining charge transfer in terms of atomic orbitals, where the charge-transfer term decreases with the basis set size and vanishes in the complete basis set limit.

The calculated charge-transfer energy in water dimer, 0.8 kcal/mol, is in good agreement with the most advanced calculations reported in the literature. Additional tests in a set comprising both weak and strong CT complexes indicate that the method is very robust and works consistently over a wide range of systems. The present implementation of the method supports only GGA and meta-GGA functionals; we plan to extend it to hybrid functionals in order to improve the accuracy further.

Because the method retains the favorable scaling of DFT calculations, it is applicable to large molecular systems. This has been illustrated by calculations of CT complexes of increasing size up to circumcoronene ... tetracyanoethylene.

## ASSOCIATED CONTENT

### Supporting Information

Table S1, containing the charge-transfer energies calculated using various population schemes, as well as a detailed discussion of the SAPT calculations. This material is available free of charge via the Internet at <http://pubs.acs.org>.

## AUTHOR INFORMATION

### Corresponding Author

\*E-mail: rezac@uochb.cas.cz.

### Notes

The authors declare no competing financial interest.

## ■ ACKNOWLEDGMENTS

This work is a part of the Research Project RVO 61388963 of the Institute of Organic Chemistry and Biochemistry AS CR; the development of the Cuby framework was supported by the grant P208/13/01214P from the Czech Science Foundation.

## ■ REFERENCES

- (1) Stone, A. *The Theory of Intermolecular Forces*, 2nd ed.; Oxford University Press: Oxford, 2013.
- (2) Stone, A. J.; Hayes, I. C. *Faraday Discuss. Chem. Soc.* **1982**, *73*, 19–31.
- (3) Szalewicz, K. *Wiley Interdiscip. Rev. Comput. Mol. Sci.* **2012**, *2*, 254–272.
- (4) von Hopffgarten, M.; Frenking, G. *Wiley Interdiscip. Rev. Comput. Mol. Sci.* **2012**, *2*, 43–62.
- (5) Mulliken, R. S. *J. Am. Chem. Soc.* **1952**, *74*, 811–824.
- (6) Anderson, P. W.; Lee, P. A.; Saitoh, M. *Solid State Commun.* **1973**, *13*, 595–598.
- (7) Kitaura, K.; Morokuma, K. *Int. J. Quantum Chem.* **1976**, *10*, 325–340.
- (8) Stone, A. J. *Chem. Phys. Lett.* **1993**, *211*, 101–109.
- (9) Stone, A. J.; Misquitta, A. J. *Chem. Phys. Lett.* **2009**, *473*, 201–205.
- (10) Azar, R. J.; Head-Gordon, M. *J. Chem. Phys.* **2012**, *136*, 024103.
- (11) Mo, Y.; Gao, J.; Peyerimhoff, S. D. *J. Chem. Phys.* **2000**, *112*, 5530–5538.
- (12) Khaliullin, R. Z.; Head-Gordon, M.; Bell, A. T. *J. Chem. Phys.* **2006**, *124*, 204105.
- (13) Reed, A. E.; Curtiss, L. A.; Weinhold, F. *Chem. Rev.* **1988**, *88*, 899–926.
- (14) Wu, Q.; Ayers, P. W.; Zhang, Y. *J. Chem. Phys.* **2009**, *131*, 164112.
- (15) Kaduk, B.; Kowalczyk, T.; Van Voorhis, T. *Chem. Rev.* **2012**, *112*, 321–370.
- (16) Becke, A. D. *J. Chem. Phys.* **1988**, *88*, 2547–2553.
- (17) Wu, Q.; Cheng, C.-L.; Voorhis, T. V. *J. Chem. Phys.* **2007**, *127*, 164119.
- (18) Wu, Q.; Kaduk, B.; Voorhis, T. V. *J. Chem. Phys.* **2009**, *130*, 034109.
- (19) Karthikeyan, S.; Sedlak, R.; Hobza, P. J. *Phys. Chem. A* **2011**, *115*, 9422–9428.
- (20) Ronca, E.; Belpassi, L.; Tarantelli, F. *ChemPhysChem* **2014**, *15*, 2682–2687.
- (21) Wu, Q.; Van Voorhis, T. *Phys. Rev. A* **2005**, *72*, 024502.
- (22) de la Lande, A.; Salahub, D. R. *J. Mol. Struct. THEOCHEM* **2010**, *943*, 115–120.
- (23) de la Lande, A.; Salahub, D.; Köster, A. In *Concepts and Methods in Modern Theoretical Chemistry*; CRC Press: Boca Raton, 2013; pp 201–2019.
- (24) Hirshfeld, F. L. *Theor. Chim. Acta* **1977**, *44*, 129–138.
- (25) Mulliken, R. S. *J. Chem. Phys.* **1955**, *23*, 1833–1840.
- (26) Löwdin, P.-O. *Adv. Quantum Chem.* **1970**, *5*, 185–199.
- (27) Bickelhaupt, F. M.; van Eikema Hommes, N. J. R.; Fonseca Guerra, C.; Baerends, E. J. *Organometallics* **1996**, *15*, 2923–2931.
- (28) Řezáč, J. *Cuby 4, Software Framework for Computational Chemistry*, <http://cuby4.molecular.cz/> (accessed Oct. 17, 2014).
- (29) Köster, A. M.; Geudtner, G.; Calaminici, P.; Casida, M. E.; Domínguez-Soria, V. D.; Flores-Moreno, R.; Gamboa, G. U.; Goursot, A.; Heine, T.; Ipatov, A.; Janetzko, F.; del Campo, J. M.; Reveles, J. U.; Vela, A.; Zuniga-Gutierrez, B.; Salahub, D. R. *deMon2k version 4*; Cinvestav: Mexico City, 2013.
- (30) Řezáč, J.; Lévy, B.; Demachy, I.; de la Lande, A. *J. Chem. Theory Comput.* **2012**, *8*, 418.
- (31) Köster, A. M.; Flores-Moreno, R.; Reveles, J. U. *J. Chem. Phys.* **2004**, *121*, 681–690.
- (32) Calaminici, P.; Janetzko, F.; Köster, A. M.; Mejia-Olvera, R.; Zuniga-Gutierrez, B. *J. Chem. Phys.* **2007**, *126*, 044108.
- (33) Köster, A. M.; Reveles, J. U.; Campo, J. M. del. *J. Chem. Phys.* **2004**, *121*, 3417–3424.
- (34) Furche, F.; Ahlrichs, R.; Hättig, C.; Klopper, W.; Sierka, M.; Weigend, F. *Wiley Interdiscip. Rev. Comput. Mol. Sci.* **2014**, *4*, 91–100.
- (35) *TURBOMOLE v6.5*; University of Karlsruhe and Forschungszentrum Karlsruhe GmbH, 2011.
- (36) Boys, S.; Bernardi, F. *Mol. Phys.* **1970**, *19*, 553–566.
- (37) Řezáč, J.; Riley, K. E.; Hobza, P. J. *Chem. Theory Comput.* **2011**, *7*, 2427–2438.
- (38) Řezáč, J.; Riley, K. E.; Hobza, P. J. *Chem. Theory Comput.* **2012**, *8*, 4285–4292.
- (39) Halkier, A.; Helgaker, T.; Jørgensen, P.; Klopper, W.; Koch, H.; Olsen, J.; Wilson, A. K. *Chem. Phys. Lett.* **1998**, *286*, 243–252.
- (40) Řezáč, J.; Riley, K. E.; Hobza, P. J. *Chem. Theory Comput.* **2011**, *7*, 3466–3470.
- (41) Řezáč, J.; Hobza, P. J. *Chem. Theory Comput.* **2013**, *9*, 2151–2155.
- (42) Werner, H.-J.; Knowles, P. J.; Manby, F. R.; Schütz, M.; et al. *MOLPRO, version 2010.1, A Package of Ab Initio Programs*; See also [www.molpro.net](http://www.molpro.net), 2010.
- (43) Grimme, S.; Antony, J.; Ehrlich, S.; Krieg, H. *J. Chem. Phys.* **2010**, *132*, 154104.
- (44) Grimme, S.; Ehrlich, S.; Goerigk, L. *J. Comput. Chem.* **2011**, *32*, 1456–1465.
- (45) Steinmann, S. N.; Piemontesi, C.; Delachat, A.; Corminboeuf, C. *J. Chem. Theory Comput.* **2012**, *8*, 1629–1640.
- (46) Mejía-Rodríguez, D.; Köster, A. M. *J. Chem. Phys.* **2014**, *141*, 124114.
- (47) Woon, D. E.; Dunning, T. H. *J. Chem. Phys.* **1994**, *100*, 2975.
- (48) Weigend, F.; Ahlrichs, R. *Phys. Chem. Chem. Phys.* **2005**, *7*, 3297–3305.
- (49) Jensen, F. *J. Chem. Phys.* **2001**, *115*, 9113–9125.
- (50) Turney, J. M.; Simmonett, A. C.; Parrish, R. M.; Hohenstein, E. G.; Evangelista, F. A.; Fermann, J. T.; Mintz, B. J.; Burns, L. A.; Wilke, J. J.; Abrams, M. L.; Russ, N. J.; Leininger, M. L.; Janssen, C. L.; Seidl, E. T.; Allen, W. D.; Schaefer, H. F.; King, R. A.; Valeev, E. F.; Sherrill, C. D.; Crawford, T. D. *Wiley Interdiscip. Rev. Comput. Mol. Sci.* **2012**, *2*, 556–565.
- (51) Hohenstein, E. G.; Parrish, R. M.; Sherrill, C. D.; Turney, J. M.; Schaefer, H. F. *J. Chem. Phys.* **2011**, *135*, 174107.
- (52) Haldar, S.; Kolář, M.; Sedlák, R.; Hobza, P. J. *Phys. Chem. C* **2012**, *116*, 25328–25336.
- (53) Fonseca Guerra, C.; Handgraaf, J.-W.; Baerends, E. J.; Bickelhaupt, F. M. *J. Comput. Chem.* **2004**, *25*, 189–210.